Global and Planetary Change xxx (2010) xxx–xxx

Contents lists available at ScienceDirect

Global and Planetary Change

journal homepage: www.elsevier.com/locate/gloplacha

# Changing seasonality patterns in Central Europe from Miocene Climate Optimum to Miocene Climate Transition deduced from the *Crassostrea* isotope archive

Mathias Harzhauser [a,*], Werner E. Piller [b], Stefan Müllegger [b], Patrick Grunert [b], Arne Micheels [c]

[a] Natural History Museum Vienna, Burgring 7, A-1030 Vienna, Austria
[b] Institute for Earth Sciences, University of Graz, Heinrichstraße 26, A-8010 Graz, Austria
[c] Senckenberg Forschungsinstitut und Naturmuseum, Biodiversität und Klima Forschungszentrum (LOEWE BiK-F), Senckenberganlage 25, 60325 Frankfurt, Germany

ARTICLE INFO

*Article history:*
Received 3 March 2010
Accepted 9 December 2010
Available online xxxx

*Keywords:*
paleoclimate
seasonality
Miocene Climate Optimum
Miocene Climate Transition
*Crassostrea*

ABSTRACT

The Western Tethyan estuarine oyster *Crassostrea gryphoides* is an excellent climate archive due to its large size and rapid growth. It is geologically long lived and allows a stable isotope-based insight into climatic trends during the Miocene. Herein we utilised the climate archive of 5 oyster shells from the Miocene Climate Optimum (MCO) and the subsequent Miocene Climate Transition (MCT) to evaluate changes of seasonality patterns.

MCO shells exhibit highly regular seasonal rhythms of warm-wet and dry-cool seasons. Optimal conditions resulted in extraordinary growth rates of the oysters. $\delta^{13}C$ profiles are in phase with $\delta^{18}O$ although phytoplankton blooms may cause a slight offset. Estuarine waters during the MCO in Central Europe display a seasonal temperature range of c. 9–10 °C. Absolute water temperatures have ranged from 17 to 19 °C during cool seasons and up to 28 °C in warm seasons.

Already during the early phase of the MCO, the growth rates are distinctly declining, although gigantic and extremely old shells have been formed at that time. Still, a very regular and well expressed seasonality is dominating the isotope profiles, but episodically occurring extreme climate events influence the environments. The seasonal temperature range is still c. 9 °C but the cool season temperature seems to be slightly lower (16 °C) and the warm season water temperature does not exceed c. 25 °C.

In the later MCT at c. 12.5–12.0 Ma the seasonality pattern is breaking down and is replaced by successions of dry years with irregular precipitation events. No correlation between $\delta^{18}O$ and $\delta^{13}C$ is documented maybe due to a suboptimal nutrition level which would explain the low growth rates and small sizes. The amplitude of seasonal temperature range is decreasing to 5–8 °C. No clear cooling trend can be postulated for that time as the winter season water temperatures range from 15 to 20 °C. This may point to unstable precipitation rhythms on a multi-annual to decadal scale as main difference between MCO and MCT climates in Central Europe instead of a simple temperature decline scenario.



## 1. Introduction

The Miocene witnessed the last global climate optimum, referred to as Miocene Climate Optimum (MCO; Zachos et al., 1994; Böhme, 2003; Sun and Zhang, 2008) and the Middle Miocene Climate Transition (MCT; Shevenell et al., 2004; Lewis et al., 2007) heralding the climatic deterioration that characterises the late Neogene world. In Eurasia, this climate change is accompanied by an increase of seasonality and aridity (Eronen et al., 2009; Bruch et al., 2010) and a replacement of Early to Middle Miocene broad-leaved evergreen forests by deciduous forests during the late Middle and Late Miocene (Kovar-Eder et al., 2008). In shelf areas, the climate change is recorded by a southward shift of reef systems and the retreat of thermophilous molluscs (Harzhauser and Piller, 2007). Whilst the large-scale climatic developments are well understood, few studies tried to elucidate Miocene seasonality based on individual skeletal records (e.g. Bojar et al., 2004; Brachert et al., 2006). Herein, the periodically formed calcite increments of large oyster shells are utilised to estimate Miocene seasonality. We consider seasonality as a periodically fluctuating character of a time series that describes predictable changes in sea water temperature and/or precipitation within a given year. These periodic variations are reflected by stable isotope patterns in the calcitic shell material. Each shell recorded the environmental conditions on an annual scale spanning between 11 and 41 years. Despite the problem that these records may overemphasise local conditions, they may nevertheless provide insight into various decades from the Early and Middle Miocene.

The oyster *Crassostrea gryphoides* (Schlotheim, 1813) is geologically long lived. Appearing in the Oligocene it persists up to the Pliocene in the

* Corresponding author. Tel.: +43 1 52177 240; fax: +43 1 52177 459.
*E-mail addresses:* mathias.harzhauser@nhm-wien.ac.at (M. Harzhauser), werner-piller@uni-graz.at (W.E. Piller), stefan.muellegger@uni-graz.at (S. Müllegger), patrick.grunert@uni-graz.at (P. Grunert), arne.micheels@senckenberg.de (A. Micheels).

0921-8181/$ – see front matter © 2010 Published by Elsevier B.V.
doi:10.1016/j.gloplacha.2010.12.003


**Fig. 1.** Huge *Crassostrea gryphoides* biostromes with more than 20,000 individuals formed during the MCO. The picture shows an excavation in the Austrian Korneuburg Basin from which shell C1 was taken (largest shell c. 60 cm).

entire Western Tethys (Schultz, 2001). With sizes of over 80 cm length, it is the largest Miocene bivalve in the Western Tethys Region (Fig. 1). Its modern congeners are economically important in shellfish farming. Therefore, numerous studies focused on the biology and ecology of *Crassostrea* including several sclerochronological studies (e.g. Hong et al., 1995; Kirby et al., 1998; Kirby, 2000; Surge et al., 2001; 2003; Higuera-Ruiz and Elorza, 2009; Lartaud et al., 2009a).

## 2. Materials and methods

The sampling protocol follows the suggestions of Kirby et al. (1998) Five left valves of *Crassostrea gryphoides* were analysed for their isotopic ($\delta^{13}C$, $\delta^{18}O$) composition. The shells were cleaned with a brush and then cut with a rock saw parallel to their maximum growth direction through the ligament area. Samples for isotopic analysis were gained by drilling a profile with a 0.3 mm-diameter dental drill near the ligament surface, perpendicular to growth increments (average distance = 0.7 mm) (Fig. 2). The ligament area has been chosen due to the results by Kirby et al. (1998) and Surge et al. (2001) who documented that in the ligament area of oysters the calcite is best preserved. The sampling area was examined with a scanning electron microscope (SEM) to evaluate the occurrence of diagenetic alteration. For SEM analysis the sample surface was polished and then treated with 0.1 N HCl for 10 s to gain crystallite growth patterns. The surface was coated with Gold–Palladium for 200 s and studied in a Zeiss DSM 982 Gemini (Fig. 2). The foliated ligament area was used in our study as no obvious diagenetic alteration was visible in this part of the shell. Samples were taken in ontogenetic growth direction. Between 36 and 206 samples per shell were gained. Isotopic analyses were performed in the Stable Isotope Laboratory at the Institute of Earth Sciences, University of Graz, using an automatic Kiel II preparation line and a Finnigan MAT Delta Plus mass spectrometer. Samples were dried and reacted with 100% phosphoric acid at 70 °C. International standard NBS-19 and an internal laboratory standard were analysed continuously for accuracy control. Standard deviation was less than 0.1‰ for $\delta^{18}O$ and 0.05‰ for $\delta^{13}C$. Isotopic data are reported in conventional δ notation relative to the Vienna Peedee belemnite (V-PDB) standard in ‰ units. All data are available as supplemental file *Crassostrea*.xls and depicted in Figs. 3 and 4.

Calculated paleotemperatures of sea water are based on the equation of Epstein et al. (1953); the estimation of the salinity regime is based on the equation of Fairbanks et al. (1992).

Shell C1 16.2 Ma (±0.1), late Burdigalian (late Early Miocene); Korneuburg Basin, Austria (N 48° 22′ 01″, E 16° 21′ 36″); length: 43 cm, width: 10 cm. The shell derives from a huge oyster biostrome consisting of more than 20.000 individuals, which had formed along sand-shoals in an estuary (Kern et al., 2010).

Shell C2 c. 15.3 Ma (±0.3), Langhian (Middle Miocene); Siegenfeld, Vienna Basin, Austria (N 48° 02′ 05″, E 16° 10′ 21″); length: 63 cm, width: 12 cm. The paleoenvironment was a western embayment of the southernVienna Basin reaching few km onto the Alpine nappes, called Gaaden Bay. There, the sandy-marly coasts were fringed by extensive *Isognomon-*, *Crassostrea-*, and *Ostrea*-biostromes (Wessely, 2006).

Shell C3 c. 14.0 Ma (±0.2), late Langhian (Middle Miocene); Poysdorf, Vienna Basin, Austria (no detailed locality data); length: 78 cm, width: 23 cm. This sample is one of the largest specimens of *Crassostrea gryphoides* found so far. The oyster was found in sandy deposits that formed on a small island few km off the coast during the Middle Miocene (Grill, 1968).

Shell C4 c. 12.4 Ma (±0.1), Serravallian (Middle Miocene); Hernals, city of Vienna, Austria (N 48° 13′ 46″, E 16° 19′ 42″); length:

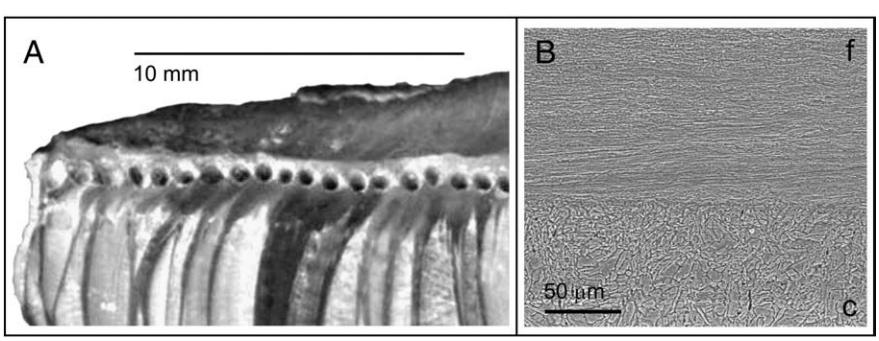


**Fig. 2.** A. Radial section of *Crassostrea gryphoides* (shell C4) documenting the sampling procedure. Samples were drilled beneath ligamental area surface. B. SEM analysis of the sample C5 showing the crystallite growth patterns of the foliate layer (f) and chalky structure (c) (sensu Ullmann et al., 2010).

Please cite this article as: Harzhauser, M., et al., Changing seasonality patterns in Central Europe from Miocene Climate Optimum to Miocene Climate Transition deduced from the Crassostrea isotope archive, Glob. Planet. Change (2010), doi:10.1016/j.gloplacha.2010.12.003

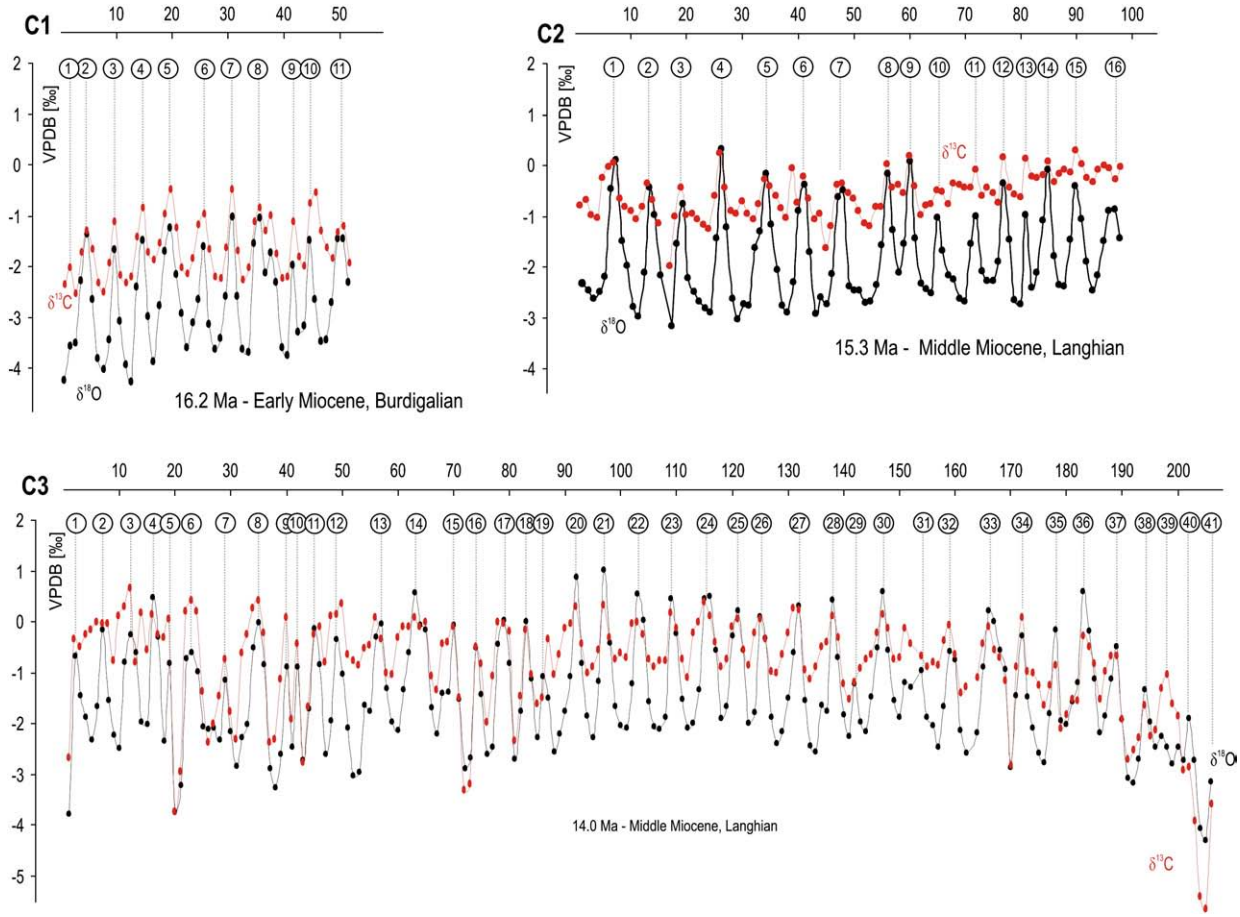


**Fig. 3.** Sclerochronological stable isotope profile ($\delta^{18}O$, $\delta^{13}C$) of the Burdigalian shell C1 and the Langhian shells C2 and C3 of *Crassostrea gryphoides*; numbers indicate the cool season. All oysters reflect very regular seasonality patterns.

14 cm, width: 7 cm). The locality, at the western margin of the Vienna Basin, represents a muddy littoral environment directly at the coast formed by Alpine nappes. No influx of a major river is recognisable here (Harzhauser and Piller, 2004).

Shell C5 c. 12.2 Ma (±0.1), Serravallian (Middle Miocene); Leobersdorf, Vienna Basin, Austria (N 47° 54′ 46″, E 16° 19′ 42″); length: 12 cm, width: 5 cm. The coastal paleoenvironment was in the sphere of influence of the paleo-Triesting river delta (Harzhauser and Piller, 2004).

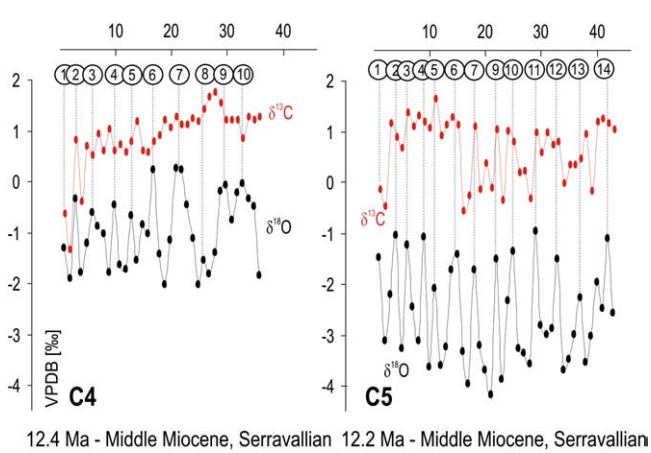


**Fig. 4.** Sclerochronological stable isotope profile ($\delta^{18}O$, $\delta^{13}C$) of the Serravallian shells C4 and C5 of *Crassostrea gryphoides*; numbers indicate the cool season. Especially the $\delta^{13}C$ show little regularity.

## 3. Results

In the following we describe the stable isotope values of all investigated shells with focus on minima and maxima but also on mean minima and mean maxima which are calculated to dampen extreme values.

Shell C1 52 sampling points; oxygen and carbon values show both a regular, serrated pattern with well defined minima and maxima and a very slight trend towards heavier values during ontogeny. $\delta^{18}O$ minima: −4.30‰ to −3.35‰; mean: −3.70‰ ($\sigma$ = 0.53); maxima: −1.04‰ to −2.06‰; mean: −1.53‰ ($\sigma$ = 0.31). The maximum range between minima and maxima is 3.26‰ and 2.17‰ between the mean values. $\delta^{13}C$ values minima: −2.57‰ to −1.95‰; mean: −2.20‰ ($\sigma$ = 0.24); maxima: −1.24‰ to −0.49‰; mean: −1.02‰ ($\sigma$ = 0.45). The total range is 3.06‰ and 1.18‰ between mean values.

Shell C2 98 sampling points; the oxygen values form a very regular serrated pattern without any trend or outliers. $\delta^{18}O$ minima: −3.21‰ to −2.49‰; mean: −2.71‰ ($\sigma$ = 0.30); maxima: −1.05‰ to 0.27‰; mean: −0.46‰ ($\sigma$ = 0.42). The total range of $\delta^{18}O$ is 3.48‰ and 2.25‰ between mean values. $\delta^{13}C$ values are less regular and show a slight trend towards heavier values during ontogeny. Most minima range between −1.28‰ and −0.32‰ except for two negative excursions (samples 17, 45); mean: −0.85‰ ($\sigma$ = 0.46). The $\delta^{13}C$ maxima have a broad range from −0.73‰ to 0.25‰; mean: −0.20‰ ($\sigma$ = 0.29). The total range in carbon values is 2.27‰ and 0.65‰ between mean values.

Please cite this article as: Harzhauser, M., et al., Changing seasonality patterns in Central Europe from Miocene Climate Optimum to Miocene Climate Transition deduced from the Crassostrea isotope archive, Glob. Planet. Change (2010), doi:10.1016/j.gloplacha.2010.12.003

Shell C3 206 sampling points; the oxygen values of this large data set form a quite regular, serrated pattern without marked trend during most of the ontogeny; only in the latest stage of growth, the values decrease abruptly to very negative values. Before that phase, $\delta^{18}O$ minima range between −3.78‰ and −1.87‰ and finally decrease to −4.28‰; mean: −2.47‰ ($\sigma$=0.48). Maxima: −1.23‰ to 1.01‰; mean: −0.23‰ ($\sigma$=0.70). The total range of $\delta^{18}O$ is 5.29‰ and 2.24‰ for mean values. The carbon values generally form a quite regular serrated pattern as well. Exceptions are distinct negative outliers (samples 20, 72, 170, 205). The trend towards strongly negative values in the latest ontogenetic stage is parallel to the oxygen values. Except for these outliers, the minima range between −2.71‰ and −0.74‰; mean: −1.63‰ ($\sigma$=0.83). The maxima are more regular and range between −0.75‰ and 0.64‰; mean: −0.09‰ ($\sigma$=0.45). The total range of $\delta^{13}C$ is 6.29‰ and 1.54‰ for mean values.

Shell C4 36 sampling points; the ontogentic pattern formed by the oxygen values is only moderately regular; especially the maxima are irregular during late stages of growth. Minima: −1.53‰ to −2.01‰; mean: −1.76‰ ($\sigma$=0.23). Distinct maxima range from −0.66‰ to 0.28‰; mean: −0.20‰ ($\sigma$=0.36). The total range is 2.29‰ and 1.56‰ for mean values. Carbon values display no regularity. Early stages of growth correlate with very negative values (−1.36‰). After sample 4, a rather narrow range of values is observed ranging between 0.49‰ and 1.72‰. The mean of the minima is 0.46‰ ($\sigma$=0.73) and 0.90‰ ($\sigma$=0.60) for the maxima. The range between mean values is 0.44‰ and 3.08‰ for the total carbon data.

Shell C5 43 sampling points; a regular serrated profile of oxygen values is formed by minima ranging from −4.18‰ to −2.51‰ and maxima ranging from −2.27‰ to −0.95‰. The mean minimum value is −3.49‰ ($\sigma$=0.44) and −1.46‰ ($\sigma$=0.40) for the maxima. No trend is visible from the data; the total range is 5.13‰ and 2.03‰ for the mean values. This regularity is absent in the carbon record which starts with a plateau of heavy maxima and minima and a sudden drop of the minima towards negative values causing a strongly serrated pattern thereafter. The minima range between −0.59‰ and 1.04‰ and the more stable maxima from 0.34‰ to 1.60‰. The mean of the minima is 0.18‰ ($\sigma$=0.61) and 1.05‰ ($\sigma$=0.30) for the maxima resulting in a range between the mean values of 0.87‰ (and a maximum range of 2.18‰).

## 4. Discussion

$\delta^{18}O$ profiles of various extant *Crassostrea* species have been documented to reliably reflect seasonal growth and seawater temperature variation. The incorporated values form close to equilibrium with the ambient seawater (Kirby et al., 1998; Surge et al., 2001; Lartaud et al., 2009a, b; Ullmann et al., 2010). Seasonality is generally indicated by regularly serrated isotope profiles. Negative $\delta^{18}O$ values indicate warmer water temperatures or a decrease in salinity during wet seasons or a combination of both. More positive values point to cooler temperatures and/or increased salinity during the drier season. This general rule of thumb was shown to be also valid for $\delta^{13}C$ (Surge et al., 2001) although the interpretation of carbon is much more complex due to the combination of seawater-derived carbon, the incorporation of organic carbon sources and various metabolic and kinetic effects (Gillikin et al., 2007; McConnaughey and Gillikin, 2008; Lartaud et al., 2009a). Thus, based on the oxygen profiles, the individual ages of the analysed shells can be estimated (cf. Kirby et al., 1998; Kirby, 2000). Based on the seasonal pattern, the minimum and maximum values can be used to calculate the paleotemperatures and to estimate the seasonal temperature range. Due to growth cessation, however, the isotope record in many modern congeners does often not reflect the full temperature ranges to which the living animal has been exposed (Ullmann et al., 2010). Growth cessation of *Crassostrea* was reported to appear either at low temperatures during winter at around 10–11.5 °C (Hong et al., 1995; Kirby, 2000) or at summer temperatures exceeding 28 ± 2 °C (Surge et al., 2001). In both cases, the $\delta^{18}O$ profiles show a characteristic pattern of truncated peaks which indicate growth cessation.

A much more severe pitfall for the calculation of the paleotemperatures is the paleogeographic setting. The Paratethys Sea was an epicontinental sea with a complex history of connections and phases of isolation from the Western Tethys (Rögl, 1998). Even within the Paratethys, the water body was not uniform due to changing sea level and geodynamics (Popov et al., 2004). This resulted in different salinities and different deviations from the Miocene SMOW (Latal et al., 2006). Moreover, the $\delta^{18}O_{w\text{-}Paratethys}$ was strongly changing between positive and negative values throughout the Miocene (Harzhauser et al., 2007). Estimations on alkalinity are similarly complex and suggest phases of increased alkalinity at least during the Sarmatian stage based on carbonate sedimentology (Piller and Harzhauser, 2005) and stable isotopes (Latal et al., 2004; Harzhauser et al., 2007). Therefore, it is extremely complex to calculate the temperature at which the carbonate was precipitated as $\delta^{18}O_w$ has to be known in the classical equation of Epstein et al. (1953). Latal et al. (2006) and Harzhauser et al. (2007) tried to overcome this problem by integrating minimum SST values derived from proxy data into the equations to estimate the deviation from the $SMOW_{Miocene}$. A similar approach was proposed by Kirby (2000) who used estimated minimum growth temperature of 10 °C as boundary condition to calculate Oligocene $\delta^{18}O_w$. In the following, each shell is interpreted in respect to seasonality and exceptional events. The paleotemperature of the water is calculated based on the $\delta^{18}O_{w\text{-}Paratethys}$ given in Latal et al. (2006) and Harzhauser et al. (2007). The results have to be used with caution due to the manifold uncertainties. Nevertheless, the estimations will result in reasonable approximations. Oysters lack photosynthetic symbionts such as the giant clam *Tridacna* (Romanek and Grossman, 1989). Therefore, the minor influence of symbiont activity on the $\delta^{13}C$ values of *Tridacna* (Elliot et al., 2009) can be excluded.

### 4.1. An oyster's life and Miocene seasons

C1 This shell exhibits the most regular annual rhythm of the studied specimens and reflects at least 11 cool seasons (Fig. 3). The seasonal temperature range between mean minima and maxima is 9.8 °C. The mean minimum temperature based on $\delta^{18}O$ maxima and on a slightly negative $\delta^{18}O_{w\text{-}Paratethys}$ ranges around 17 °C which is close to estimates of 13–16 °C in Latal et al. (2006) and 14–16 °C in Harzhauser et al. (2002). Highest recorded summer temperatures would attain c. 27 °C which is close to the summer growth cessation temperature of 28 ± 2 °C of extant congeners (Surge et al., 2001). The strong seasonality signal in temperature fits well to estimations of Böhme et al. (2007; Böhme, 2010) and Kern et al. (2010) who reconstruct a pronounced dry season for the latest Burdigalian of Central Europe. The salinity ranges around 23 psu which fits to the position of the oyster reef within the proximal part of the estuary.

C2 Seasonality in temperature is clearly expressed by the regular $\delta^{18}O$ pattern (Fig. 3); at least 16 years are recorded with a seasonal temperature range of 9 °C. Based on a positive $\delta^{18}O_{w\text{-}Paratethys}$ for the early Langhian the minimum temperature to which the oyster was exposed is c. 19 °C. Growth might have stopped at the maximum temperature of 28 °C indicated by

truncated summer troughs (summer 3) whilst growth was continuous in years with slightly cooler summer temperatures (summer 7). The rather high hypothetical salinity of 39 psu might be overestimated. A generally elevated salinity, however, would fit to the paleogeographic situation in an enclosed marine lagoon without freshwater input. This setting explains also the low range of carbon values and the lack of a marked seasonality signal which would be expected under seasonal freshwater input. Moreover, the $\delta^{13}C$ amplitudes are decreasing throughout ontogeny and a trend towards heavier values is evident. That points to a decreasing input of isotopically light DIC and takeover by marine conditions. In addition, the geological basement consisting of largely Mesozoic carbonates might additionally have supported elevated $\delta^{13}C$ levels.

C3 The extremely long record of C3 gives insight into 4 decades of early Middle Miocene climate (Fig. 3). The range between the total mean minima and mean maxima suggests a temperature range of 8.4 °C. Based on a positive $\delta^{18}O_{w\text{-}Paratethys}$ of about 1.2 for the middle Langhian a winter water temperature of c. 16 °C can be calculated and a summer temperature around 25 °C.

The data set can be separated into discrete phases. The first lasts up to years 15–16 and is characterized by rather irregular rhythms, large amplitudes and irregular minima. The temperature range of that interval is c. 16 °C. The low minima might hint to several years of high freshwater input. This is supported by the simultaneous excursions in $\delta^{13}C$ (years 5–8, 15). The potential source for that freshwater input was a delta some km west of the island (Wessely, 2006). After that phase, a rather uniform and regular seasonal rhythm up to the year 33 is reflected by the isotope pattern. Uniform minima and maxima suggest a seasonal temperature range of c. 12 °C. Exceptional maxima in the years 20 and 21 might reflect evaporation effects during the dry and hot season.

Similar aberrations, due to "extreme-climate-events" have been documented by Schöne et al. (2005) from sclerochronological profiles of extant *Arctica islandica*. Strongly negative excursions in $\delta^{18}O$ and $\delta^{13}C$ in years 33, 37 and 40 might suggest an increased frequency of freshwater discharge events as documented for fossil and extant molluscs by Tripati et al. (2001) and Khim et al. (2003). These are explained by the contribution of isotopically light freshwater with soil derived carbon (Leng and Marshall, 2004).

A decrease of $\delta^{13}C$ during ontogeny and especially in late stages of growth has been frequently observed in sclerochronologic studies (Gillikin et al., 2007; McConnaughey and Gillikin, 2008) This phenomenon is explained by a preferred uptake of light metabolic carbon with increased age and enhanced reproductivity (Lorrain et al., 2004; Lartaud et al., 2009a). In our data set only shell C3 displays a trend towards depleted $\delta^{13}C$ values in the latest stage of growth. Even, if the extremely negative samples 170, 204 and 205 are excluded as these are rather related to freshwater events, a general decrease of values starts after sample 147 during the last decade of the oyster's life. This pattern in the giant shell C3 fits to the observation of Lorrain et al. (2004) and Gillikin et al. (2007) that the contribution of metabolic carbon increases with size and age of certain bivalve taxa. Consequently, the much smaller and less aged shells lack this downshift trend. Although the carbon values of the last years in C3 might thus be influenced by metabolic effects, the parallel trend of the oxygen values suggest a general increase of freshwater input.

Carbon isotope patterns are not completely in phase with oxygen isotopes. Although the maxima usually coincide, the increase of $\delta^{13}C$ values predates the $\delta^{18}O$ values (e.g. years 2/3, 7/8, 12/13, 13/14, and 19/20). This suggests that water was enriched in $\delta^{13}C$ during phytoplankton blooms in autumn and comparatively depleted in spring. Phytoplankton preferentially incorporates light $^{12}C$ and thus enriches the ambient water in $^{13}C$. Subsequent decay recycles the light carbon into the water and decreases $\delta^{13}C$ values. A comparable scenario with spring blooms was described by Hong et al. (1995) from Holocene *Crassostrea*.

C4 The pattern is rather irregular; recorded winter temperatures are strongly fluctuating and seem to represent 10 years of growth (Fig. 4). In contrast, the warm season signal is fairly constant. The calculated coldest temperatures, based on a slightly positive $\delta^{18}O_{w\text{-}Paratethys}$, range around 15 °C, but the range between mean minima and maxima is only c. 5 °C. The summer temperature reached c. 23 °C. $\delta^{13}C$ values are very high and show no clear phase relation with $\delta^{18}O$. No growth limitation is to be expected within that temperature range and thus no cessation is indicated by the isotope values. During the first year, the shell documents a sudden increase from negative isotope values towards heavy values, which then display little fluctuation and lack seasonality signals. Influx of $^{12}C$ by rivers is very low. This pattern points to a rather stable $^{13}C$ pool and fits to a low precipitation and high alkalinity scenario as proposed by Piller and Harzhauser (2005), Harzhauser et al. (2007) and Böhme et al. (2008). The elevated values are also reflected in the salinity calculations of c. 30 psu.

C5 The seasonality signal is well expressed by a regular pattern of $\delta^{18}O$, indicating about 14 cool seasons (Fig. 4). The calculated winter temperature is rather high and ranges around 20 °C. The range between the mean minima and maxima is c. 8 °C. A growth cessation due to high summer temperatures is not expressed in the data and thus the summer temperatures seem to have stayed below 28 °C. Salinity ranged around 30 psu. As in C4, the correlation with carbon isotope values is poor due to a frequent offset of the $\delta^{13}C$ maxima. Seasonality signals are indistinct in the $\delta^{13}C$ record. After a sudden increase in the first year, a first plateau phase is established up to year 6. Afterwards, the amplitudes increase and the maxima are slightly better correlated with the $\delta^{18}O$ maxima. As the $\delta^{18}O$ minima show a shift towards more negative values at the turning point from the high $\delta^{13}C$ plateau towards the high amplitude carbon record, this might reflect an irregular increase of freshwater input during the warm season.

### 4.2. Patterns and trends

Numerous studies on extant *Crassostrea* have proven that the stable isotope profiles of the shells reliably reflect seasonal changes in temperature, salinity and other environmental parameters (Hong et al., 1995; Kirby et al., 1998; Kirby, 2000; Surge et al., 2001, 2003; Higuera-Ruiz and Elorza, 2009; Lartaud et al., 2009a). To analyse the stability of the seasonality signal in the isotope data time series analysis was applied using the software package "Past" (Hammer et al., 2001).

Two shells did form during the MCO: the latest Burdigalian shell C1 and the early Langhian shell C2. Both display very regular seasonality signals and quite stable ranges in both stable isotopes. They reflect higher summer temperatures than C3 which lived already during the MCT and are also outstanding in their growth rates (Fig. 5). This fits well to the observation of Cáceres-Puig et al. (2007) that higher temperatures support growth rates of *Crassostrea*. The latest Langhian MCT shell C3 exhibits still a very clear seasonal signal but reflects several aberrations which might have been caused by freshwater discharge events and dry years.

The analyses of the power spectra of the oxygen data of all three shells reveals clear seasonality signals with distinct peaks above the 95% confidence interval (Fig. 6).

Please cite this article as: Harzhauser, M., et al., Changing seasonality patterns in Central Europe from Miocene Climate Optimum to Miocene Climate Transition deduced from the Crassostrea isotope archive, Glob. Planet. Change (2010), doi:10.1016/j.gloplacha.2010.12.003

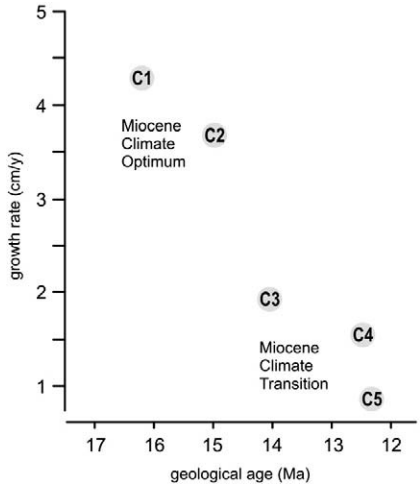


**Fig. 5.** Growth rates of the oysters based on their ontogenetic age in relation to their size. The shells that grew during the MCO (C1, C2) have much higher growth rates than those from the MCT (C3, C4, and C5).

The Serravallian MCT shells C4 and C5, however, lack any statistically relevant signal and do not show clear seasonality peaks. Moreover, the $\delta^{13}C$ profiles of the two shells suggest a generally low precipitation during the late Serravallian occurring in irregular sequences. Up to 5 to 10 years lasting draughts are indicated by the stable isotope profiles. Suboptimal conditions are also indicated by the size of these shells (and all other Sarmatian *Crassostrea*) which do never reach the size of the Burdigalian and Langhian ones The poor seasonality signal may thus be explained by rather low and irregular precipitation between 12.5 and 12.3 Ma in Central Europe. This trend seems to have climaxed at c. 12.0 Ma when oolite shoals start to spread in the entire Paratethys Sea (Piller and Harzhauser, 2005). At that time, however, *Crassostrea* became extinct from the Paratethys, and no oyster-shell isotope record can be measured. Nevertheless, strong evaporative effects have been postulated for that phase by Latal et al. (2004) based on stable isotopes from aragonitic molluscs.

The investigated shells display two general modes of $\delta^{18}O/\delta^{13}C$ correlation. The MCO shells C1, C2 and the early MCT shell C3 exhibit a highly significant positive correlation (C1: $r^2 = 0.74$; $p = 0.001$; C2: $r^2 = 0.48$; $p = 0.001$; C3: $r^2 = 0.54$; $p = 0.001$). The late MCT shells lack such a correlation (C4: $r^2 = 0.05$) or show a distinctly lower value (C5: $r^2 = 0.31$). The isotope coupling occurs as result of water temperatures depending increase of metabolic activity enabled by high nutrient availability (Lartaud et al., 2009a). Moreover, the simple input of isotopically light carbon with seasonally increased freshwater influx would cause a coupling of both isotopes. The lack of correlation is thus influenced by a lack of such events. Moreover, Lartaud et al. (2009a) demonstrated a lack of $\delta^{18}O/\delta^{13}C$ correlation at low food rations whereas high food rations in experimentally reared *Crassostrea gigas* resulted in a high correlation. The combination of both effects may thus have influenced the isotope values of the late MCT shells C4 and C5. Low nutrition in coastal areas of the late Serravallian Paratethys Sea, would also explain the small shell size during that time. Dry seasons may strongly elevate $\delta^{18}O$ values in estuaries due to evaporation (Surge and Lohmann, 2002). This phenomenon may have caused the positive excursions in $\delta^{13}C$. In contrast, freshwater input by exceptional floods or precipitation will cause strongly negative $\delta^{18}O$ excursions as seen in C3. These events are accompanied by negative shifts of $\delta^{13}C$ as typical signal of increased freshwater input (Surge and

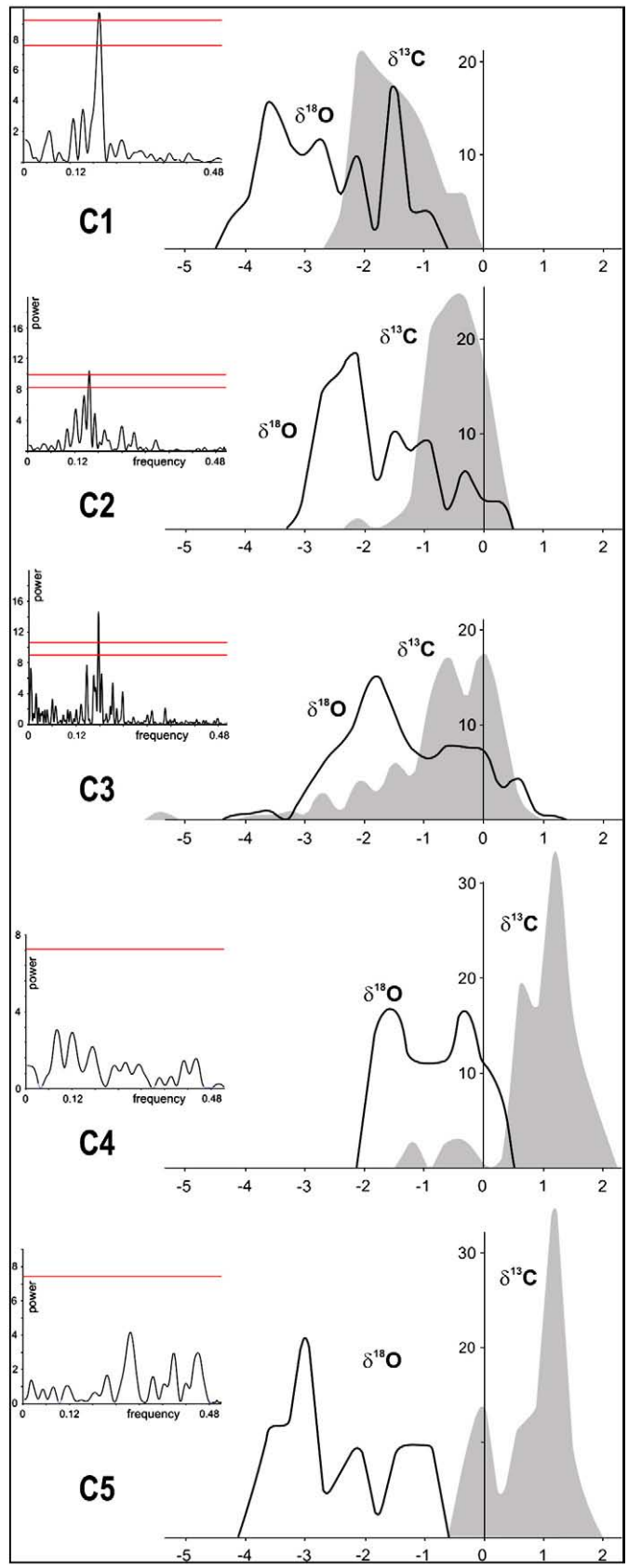


**Fig. 6.** Frequency diagrams of observed $\delta^{18}O$ and $\delta^{13}C$ values in 5 Miocene time series (black line $\delta^{18}O$; grey field $\delta^{13}C$; frequencies are given in %). Note the shift towards positive $\delta^{13}C$ values in the Serravallian shells C4 and C5. The power spectra of the oxygen data clearly indicate a well expressed seasonal peak in shells C1, C2 and C3 but a loss of that signal in C4 and C5 (red lines are 90 and 95% confidence intervals). (For interpretation of the references to color in this figure legend, the reader is referred to the web version of this article.)

Please cite this article as: Harzhauser, M., et al., Changing seasonality patterns in Central Europe from Miocene Climate Optimum to Miocene Climate Transition deduced from the Crassostrea isotope archive, Glob. Planet. Change (2010), doi:10.1016/j.gloplacha.2010.12.003

Lohmann, 2002). Hence, $\delta^{13}C$ is frequently used as paleo-salinity proxy because freshwater DIC is isotopically lighter than marine DIC due to the $CO_2$ contribution from decomposed terrestrial plants (McConnaughey and Gillikin, 2008). In estuaries, this contribution by litter may cause more negative values than expected even for the seawater end member (Surge and Lohmann, 2002). Again, the low carbon ranges and high values during the late MCT indicate a predominance of isotopically heavy marine DIC as result of the absence of dilution by land-derived light DIC. Regularly occurring phytoplankton blooms can be excluded based on the $\delta^{13}C$ isotope profiles, which is another hint to a lowered nutrient availability.

Our data demonstrate a loss of the clear annual signal after the early Middle Miocene (Fig. 5). This points to increased inter-annual climate variability. A possible mechanism, which explains our results, can be a more frequent and/or more intense cyclone activity in the North Atlantic and European realm in the Serravallian. A Late Miocene coral record from Greece supports that the eastern Mediterranean climate has been linked to conditions in the North Atlantic region (Brachert et al., 2006). Böhme et al. (2008) suggested a climatic teleconnection of the Atlantic and the European region in the Late Serravallian and Tortonian. They demonstrated that conditions in Central and Eastern Europe became more humid during the Serravallian. In contrast, a change of the mammal fauna of the E-Mediterranean starting in the late Middle Miocene indicates a trend of increasingly drier conditions towards the Late Miocene (Eronen et al., 2009). Both studies, Böhme et al. (2008) and Eronen et al. (2009), document a shift of precipitation patterns in Europe from the Serravallian to the Tortonian. A climate model experiment for the Late Miocene, too, demonstrated increased precipitation compared to today in Central Europe and drier-than-present conditions in the Mediterranean area (Micheels et al., 2010). These changed precipitation patterns are related to intensified westerlies in the North Atlantic and European realm. The more intense westerlies represent an increased stormtrack activity (Micheels et al., 2010), which fits with our findings of increased inter-annual climate variability. Increased climate variability in the western part of the Paratethys might not only be related to the Atlantic region, but might also be caused by internal Paratethyan parameters. The heat capacity of land and ocean differs. Hence, the retreat of the Paratethys from the Early to the Middle Miocene led to a successively reduced damping effect of the water body. Climate modelling sensitivity experiments demonstrated that the shrinkage of the Paratethys during the Miocene had an influence on the regional climate and on the global circulation (Ramstein et al., 1997; Fluteau et al., 1999). Ramstein et al. (1997) suggested that the Paratethys retreat led to a more continental climate in the Middle-to-Late Miocene and to the formation of the Siberian high in winter. An increased seasonality due to the shrinkage of the Paratethys in the model experiments (Ramstein et al., 1997; Fluteau et al., 1999) is consistent to our data. It is not an easy task to unravel the climate mechanisms from our data and our results should not be overestimated. However, our records represent the general climate cooling in the Miocene and the most striking feature is that they indicate an increased variability on a short time-scale during the transition into the Middle Miocene. Usually, higher frequency patterns for Miocene time intervals are beyond the temporal resolution of other proxy data (e.g., Mosbrugger et al., 2005).

## 5. Conclusions

*Crassostrea gryphoides* is the largest Western Tethyan Miocene mollusc known to date and individual ontogenetic ages of several decades are frequently observed. Due to its size, its regular growth increments can be studied easily in cross sections of the ligament area. Aside from corals, this mollusc is therefore the most suitable organism to monitor Miocene climate and especially seasonality patterns over several years in the past. The calcitic shell-chemistry of the bivalve is a further advantage over aragonitic skeletons of other bivalves, gastropods and corals which are easily prone to chemical alterations. The bivalve was a specialist for estuarine habitats, which, as junction between terrestrial and marine environments, are strongly modulated by climatic parameters such as precipitation and discharge. Seasonal rhythms of the climate may thus be detected from the *Crassostrea* isotope archive. The wide paleogeographic distribution of that bivalve from the eastern Atlantic to the western Indo-Pacific and its long geological persistence from the Oligocene to the Pliocene indicates *C. gryphoides* as key organism for studies on mid-Cenozoic seasonality.

The analysed shells of the giant oyster *Crassostrea gryphoides* document a distinct change in seasonality patterns from the Miocene Climate Optimum (MCO) into the Miocene Climate Transition (MCT). The Burdigalian and Langhian shells exhibit a markedly regular seasonality with regularly occurring seasons of high precipitation, reflected by increased freshwater discharge into the estuaries. Individual growth rates are about 2–3 times faster than in geologically younger oysters in the Paratethys Sea. In contrast to the MCO shells, with parallel $\delta^{18}O$ and $\delta^{13}C$ profiles, the early MCT shell indicates phytoplankton blooms during autumn, reflected by a slight phase lag. MCO water temperatures ranged between 17 and 19 °C during cool seasons and c. 28 °C in warm seasons with a characteristic seasonal range of 9–10 °C. The extremely long 4-decade-record of the huge oyster from the early MCT still suggests a strong seasonality. A slight cooling might be expressed by the annual temperature range from c. 16–25 °C. Soon after, the Serravallian shells of Central Europe document a drastic change of patterns. Successions of dry years with irregular precipitation events occur, whereas the $\delta^{18}O$ record suggests a continuous regular alternation of warm and cool seasons. The breakdown of isotope correlation may thus be related to suboptimal nutrition supply which would also explain the small shell-sizes during that time.

In terrestrial climates the MCO/MCT transition is characterized by an increase in mean annual range of temperature, mainly due to decreasing cold month temperatures (Böhme, 2003; Mosbrugger et al., 2005; Bruch et al., 2010). This trend is not so obvious in the data presented here for the shells from the late MCT. Rather warm Paratethyan sea water temperatures during the late Serrvallian, however, are also indicated by the wide spread ooid formation, which contradicts a pronounced cooling at that time (Piller and Harzhauser, 2005). Therefore, unstable precipitation on a multi-annual to decadal scale, rather than a simple temperature decline, may thus be an important forcing mechanism for the MCT climate in Central Europe.

## Acknowledgments

This paper was financially supported by the Commission for Palaeontological and Stratigraphical Research of Austria of the Austrian Academy of Sciences. It contributes to the NECLIME project and is part of the Austrian Science Foundation project FWF-grants P21414-B16. Arne Micheels was supported by the Deutsche Forschungsgemeinschaft (DFG) within the project FOR 1070 and the federal state Hessen (Germany) within the LOEWE initiative.

## Appendix A. Supplementary data

Supplementary data to this article can be found online at doi:10.1016/j.gloplacha.2010.12.003.

## References

Böhme, M., 2003. Miocene Climatic Optimum: evidence from lower vertebrates of Central Europe. Palaeogeography, Palaeoclimatology, Palaeoecology 195, 389–401.
Böhme, M., 2010. Ectothermic vertebrates (Actinopterygii, Allocaudata, Urodela, Anura, Crocodylia, Squamata) from the Miocene of Sandelzhausen (Germany, Bavaria) and

their implications for environment reconstruction and palaeoclimate. Paläontologishe Zeitscrift 84, 3–42.
Böhme, M., Bruch, A.A., Selmeier, A., 2007. The reconstruction of Early and Middle Miocene climate and vegetation in Southern Germany as determined from the fossil wood flora. Palaeogeography, Palaeoclimatology, Palaeoecology 253, 91–114.
Böhme, M., Ilg, A., Winkelhofer, M., 2008. Late Miocene "washhouse" climate in Europe. Earth and Planetary Science Letters 275, 393–401.
Bojar, A.-V., Hiden, H., Fenninger, A., Neubauer, F., 2004. Middle Miocene seasonal temperature changes in the Styrian basin, Austria, as recorded by the isotopic composition of pectinid and brachiopod shells. Palaeogeography, Palaeoclimatology, Palaeoecology 203, 95–105.
Brachert, T.C., Reuter, M., Felis, T., Kroeger, K.F., Lohmann, G., Micheels, A., Fassoulas, C., 2006. *Porites* corals from Crete (Greece) open a window into Late Miocene (10 Ma) seasonal and interannual climate variability. Earth and Planetary Science Letters 245, 81–94.
Bruch, A.A., Utescher, T., Mosbrugger, V., NECLIME members, 2010. Precipitation patterns in the Miocene of Central Europe and the development of continentality. Palaeogeography, Palaeoclimatology, Palaeoecology. doi:10.1016/j.palaeo.2010.10.002.
Cáceres-Puig, J.I., Abasolo-Pacheco, F., Mazón-Suastegui, J.M., Maeda-Martínez, A.N., Saucedo, P.E., 2007. Effect of temperature on growth and survival of *Crassostrea corteziensis* spat during late-nursery culturing at the hatchery. Aquaculture 272, 417–422.
Elliot, M., Welsh, K., Chilcott, C., McCulloch, M., Chappell, J., Ayling, B., 2009. Profiles of trace elements and stable isotopes derived from giant long-lived *Tridacna gigas* bivalves: potential applications in paleoclimate studies. Palaeogeography, Palaeoclimatology, Palaeoecology 280, 132–142.
Epstein, S., Buchsbaum, R., Lowenstam, H.A., Urey, H.C., 1953. Revised carbonate-water isotopic temperature scale. Geological Society of America Bulletin 64, 1315–1326.
Eronen, J.T., Mirzaie, M., Karme, A., Micheels, A., Bernor, R.L., Fortelius, M., 2009. Distribution history and climatic controls of the Late Miocene Pikermian chronofauna. Proceedings of the National Academy of Science 106, 11867–11871.
Fairbanks, R.G., Charles, C.D., Wright, J.D., 1992. Origin of global meltwater pulses. In: Taylor, E., Long, A., Kra, R.S., Taylor, E., Long, A., Kra, R.S. (Eds.), Radiocarbon After Four Decades. Springer-Verlag, New York, pp. 473–500.
Fluteau, F., Ramstein, G., Besse, J., 1999. Simulating the evolution of the Asian and African monsoons during the past 30 Myr using an atmospheric general circulation model. Journal of Geophysical Research 104, 11995–12018.
Gillikin, D.P., Lorrain, A., Meng, L., Dehairs, F., 2007. A large metabolic carbon contribution to the $\delta^{13}C$ record in marine aragonitic bivalve shell. Geochimia et Cosmochimia Acta 71, 2936–2946.
Grill, R., 1968, Erläuterungen zur geologischen Karte des nordöstlichen Weinviertels und zu Blatt Gänserndorf: Wien, Geologische Bundesanstalt, 155 p.
Hammer, Ø., Harper, D.A.T., Ryan, P.D., 2001. PAST; Palaeontological Statistics software package for education and data analysis. Palaeontologica Electronica 4, 1–9.
Harzhauser, M., Piller, W.E., 2004. Integrated stratigraphy of the Sarmatian (Upper Middle Miocene) in the western Central Paratethys. Stratigraphy 1, 65–86.
Harzhauser, M., Piller, W.E., 2007. Benchmark data of a changing sea — palaeogeography, palaeobiogeography and events in the Central Paratethys during the Miocene. Palaeogeography, Palaeoclimatology, Palaeoecology 253, 8–31.
Harzhauser, M., Böhme, M., Mandic, O., Hofmann, Ch.-C.h., 2002. The Karpatian (Late Burdigalian) of the Korneuburg Basin — a palaeoecological and biostratigraphical synthesis. Beiträge zur Paläontologie 27, 441–456.
Harzhauser, M., Piller, W.E., Latal, C., 2007. Geodynamic impact on the stable isotope signatures in a shallow epicontinental sea. Terra Nova 19, 1–7.
Higuera-Ruiz, R., Elorza, J., 2009. Biometric, microstructural, and high-resolution trace element studies in *Crassostrea gigas* of Cantabria (Bay of Biscay, Spain): anthropogenic and seasonal influences. Estuarine, Coastal and Shelf Science 82, 201–213.
Hong, W., Keppens, E., Nielsen, P., van Riet, A., 1995. Oxygen and carbon isotope study of the Holocene oyster reefs and paleoenvironmental reconstruction on the northwest coast of Bohai Bay, China. Marine Geology 124, 289–302.
Kern, A., Harzhauser, M., Mandic, O., Roetzel, R., Ćorić, S., Bruch, A.A., Zuschin, M., 2010. Millennial-scale vegetation dynamics in an estuary at the onset of the Miocene Climate Optimum. Palaeogeography, Palaeoclimatology, Palaeoecology. doi:10.1016/j.palaeo.2010.07.014.
Khim, B.-K., Krantz, D.E., Cooper, L.W., Grebmeier, J.M., 2003. Seasonal discharge of estuarine freshwater to the western Chukchi Sea shelf identified in stable isotope profiles of mollusk shells. Journal of Geophysical Research 108. doi:10.1029/2003JC001816.
Kirby, M.X., 2000. Paleoecological differences between Tertiary and Quaternary *Crassostrea* oysters, as revealed by stable isotope sclerochronology. Palaios 15, 132–141.
Kirby, M.X., Soniat, T.M., Spero, H.J., 1998. Stable isotope sclerochronology of Pleistocene and Recent oyster shells (*Crassostrea virginica*). Palaios 13, 560–569.
Kovar-Eder, J., Jechorek, H., Kvaček, Z., Parashiv, V., 2008. The integrated plant record: an essential tool for reconstructing Neogene zonal vegetation in Europe. Palaios 23, 97–111.
Lartaud, F., Emmanuel, L., de Rafelis, M., Pouvreau, S., Renard, M., 2009a. Influence of food supply on the δ13C signature of mollusc shells: implications for palaeoenvironmental reconstitutions. Geo-Marine Letters. doi:10.1007/s00367-009-0148-4.
Lartaud, F., Emmanuel, L., de Rafelis, M., Pouvreau, S., Ropert, M., Labourdette, N., Richardson, C.A., Renard, M., 2009b. A latitudinal gradient of seasonal temperature variation recorded in oyster shells from the coastal waters of France and The Netherlands. Facies. doi:10.1007/s10347-009-0196-2.
Latal, C., Piller, W.E., Harzhauser, M., 2004. Paleoenvironmental reconstruction by stable isotopes of Middle Miocene Gastropods of the Central Paratethys. Palaeogeography, Palaeoclimatology, Palaeoecology 211, 157–169.
Latal, C., Piller, W.E., Harzhauser, M., 2006. Shifts in oxygen and carbon isotope signals in marine molluscs from the Central Paratethys (Europe) around the Lower/Middle Miocene transition. Palaeogeography, Palaeoclimatology, Palaeoecology 231, 347–360.
Leng, M., Marshall, J.D., 2004. Palaeoclimate interpretation of stable isotope data from lake sediment archives. Quaternary Science Reviews 23, 811–831.
Lewis, A.R., Marchant, D.R., Ashworth, A.C., Hemming, S.R., Machlus, M.L., 2007. Major middle Miocene global climate change: evidence from East Antarctica and the Transantarctic Mountains. Geological Society of America Bulletin 119, 1449–1461.
Lorrain, A., Paulet, Y.-M., Chauvaud, L., Dunbar, R., Mucciarone, D., Fontugne, M., 2004. δ13C variation in scallop shells: increasing metabolic carbon contribution with body size? Geochimia et Cosmochimia Acta 68, 3509–3519.
McConnaughey, T.A., Gillikin, D.P., 2008. Carbon isotopes in mollusk shell carbonates. Geo-Marine Letters 28, 287–299.
Micheels, A., Bruch, A.A., Eronen, J., Fortelius, M., Harzhauser, M., Utescher, T., Mosbrugger, V., 2010. Analysis of heat transport mechanisms from a Late Miocene model experiment with a fully-coupled atmosphere-ocean general circulation model. Palaeogeography, Palaeoclimatology, Palaeoecology. doi:10.1016/j.palaeo.2010.09.021.
Mosbrugger, V., Utescher, T., Dilcher, D.L., 2005. Cenozoic continental climatic evolution of Central Europe. Proceedings of the National Academy of Science 102, 14964–14969.
Piller, W.E., Harzhauser, M., 2005. The myth of the brackish Sarmatian Sea. Terra Nova 17, 450–455.
Popov, S.V., Rögl, F., Rozanov, A.Y., Steininger, F.F., Shcherba, I.G., Kovac, M., 2004. Lithological–paleogeographic maps of Paratethys. 10 Maps Late Eocene to Pliocene. Courier Forschungsinstitut Senckenberg 250, 1–46.
Ramstein, G., Fluteau, F., Besse, J., Joussaume, S., 1997. Effect of orogeny, plate motion and land–sea distribution on Eurasian climate change over the past 30 million years. Nature 386, 788–795.
Rögl, F., 1998, Palaeogeographic considerations for Mediterranean and Paratethys Seaways (Oligocene to Miocene): Annalen des Naturhistorischen Museums in Wien 99, 279–310.
Romanek, C.S., Grossman, E.L., 1989. Stable isotope profiles of *Tridacna maxima* as environmental indicators. Palaios 4, 402–413.
Schöne, B.R., Pfeiffer, M., Pohlmann, T., Siegismund, F., 2005. A seasonally resolved bottom-water temperature record for the period AD 1866–2002 based on shells of *Arctica islandica* (Mollusca, North Sea). International Journal of Climatology 25, 947–962.
Schultz, O., 2001. Bivalvia neogenica (Nuculacea–Unionacea), in Piller, W.E., ed., Catalogus Fossilium Austriae. Wien, Akademie der Wissenschaften 1/1, 379 p.
Shevenell, A.E., Kennett, J.P., Lea, D.W., 2004. Middle Miocene Southern Ocean cooling and Antarctic cryosphere expansion. Science 305, 1766–1770.
Sun, J., Zhang, Z., 2008. Palynological evidence for the Mid-Miocene Climatic Optimum recorded in Cenozoic sediments of the Tian Shan Range, northwestern China. Global and Planetary Change 64, 53–68.
Surge, D.M., Lohmann, K.C., 2002. Temporal and spatial differences in salinity and water chemistry in SW Florida estuaries. Effects of human-impacted watersheds. Estuaries 25, 393–408.
Surge, D.M., Lohmann, K.C., Dettman, D.L., 2001. Controls on isotopic chemistry of the American oyster, *Crassostrea virginica*: implications for growth patterns. Palaeogeography, Palaeoclimatology, Palaeoecology 172, 283–296.
Surge, D.M., Lohmann, K.C., Goodfriend, G.A., 2003. Reconstructing estuarine conditions: oyster shells as recorders of environmental change, Southwest Florida. Estuarine, Coastal and Shelf Science 57, 737–756.
Tripati, A., Zachos, J., Marincovich Jr., L., Bice, K., 2001. Late Paleocene Arctic coastal climate inferred from molluscan stable and radiogenic isotope ratios. Palaeogeography, Plaeoclimatology, Palaeoecology 170, 101–113.
Ullmann, C.V., Wiechert, U., Korte, C., 2010. Oxygen isotope fluctuations in a modern North Sea oyster (*Crassostrea gigas*) compared with annual variations in seawater temperature: implications for palaeoclimate studies. Chemical Geology 277, 160–166.
Wessely, G., 2006, Niederösterreich. Geologie der österreichischen Bundesländer: Wien, Geologische Bundesanstalt Wien, 416 p.
Zachos, J.C., Stott, L.D., Lohmann, K.C., 1994. Evolution of early Cenozoic marine temperatures. Paleoceanography 9, 353–387.

Please cite this article as: Harzhauser, M., et al., Changing seasonality patterns in Central Europe from Miocene Climate Optimum to Miocene Climate Transition deduced from the Crassostrea isotope archive, Glob. Planet. Change (2010), doi:10.1016/j.gloplacha.2010.12.003